

**Dissipation-induced first-order decoherence phase transition in a noninteracting fermionic system**M. V. Medvedyeva,<sup>1</sup> M. T. Čubrović,<sup>2</sup> and S. Kehrein<sup>1</sup><sup>1</sup>*Institute for Theoretical Physics, Georg-August-Universität Göttingen, Friedrich-Hund-Platz 1, D-37077 Göttingen, Germany*<sup>2</sup>*Institute for Theoretical Physics, Universität zu Köln, Zùlpicher Str. 77, D-50937 Köln, Germany*

(Received 21 October 2014; revised manuscript received 3 February 2015; published 13 May 2015)

We consider a quantum wire connected to the leads and subjected to dissipation along its length. The dissipation manifests as tunneling into (out of) the chain from (to) a memoryless environment. The evolution of the system is described by the Lindblad equation. Already infinitesimally small dissipation along the chain induces a quantum phase transition (QPT). This is a decoherence QPT: the reduced density matrix of a subsystem in the nonequilibrium steady state (far from the ends of the chain) can be represented as the tensor product of single-site density matrices. The QPT is identified from the jump of the current and the entropy per site as the dissipation becomes nonzero. We also explore the properties of the boundaries of the chain close to the transition point and observe that the boundaries behave as if they undergo a second-order phase transition as a function of the dissipation strength: the particle-particle correlation functions and the response to the electric field exhibit a power-law divergence. Disorder is known to localize one-dimensional systems, but the coupling to the memoryless environment pushes the system back into the delocalized state even in the presence of disorder. Interestingly, we observe a similar transition in the classical dissipative counterflow model: the current has a jump at the ends of the chain introducing an infinitely small dissipation.

DOI: [10.1103/PhysRevB.91.205416](https://doi.org/10.1103/PhysRevB.91.205416)

PACS number(s): 03.65.Yz, 72.10.-d, 72.15.Rn, 05.30.Fk

**I. INTRODUCTION**

Coupling to the environment can significantly change the properties of a quantum system. Intuitively, the presence of dissipation leads to a decrease of coherence in the system. It can induce various types of phase transitions [1–9].

The best known example of such a transition is exhibited by the spin-boson model: there is a critical value of the interaction between the two-level system and the bosonic environment, which localizes the system [10]. A more complicated example is the superconductor-metal transition in dissipative nanowires [6,7], which can be modeled as a dissipative  $XY$ -spin chain, with a coupling to the bosonic bath at every site of the chain. It was shown both analytically and numerically [6,8,9] that the system experiences a universal second-order phase transition at the critical value of the coupling to the environment.

These are examples in the presence of the bosonic bath. Realistically, especially in condensed matter systems, the bath can be also fermionic [11]. It is possible to describe it in a similar manner as the bosonic bath in the spin-boson model, i.e., using the Feynman-Vernon formalism. However, it is rather complicated to consider more than one or two sites in such a formulation. The problem is often simplified by studying a Lindblad-type equation [12,13]. This corresponds to a memoryless bath. Physically, this means that the quasiparticles in the bath are assumed to have a much smaller dynamical timescale compared to the excitations in the system. Even the memoryless dissipation induces a novel behavior in the quantum systems. For example, dissipation along the system can lead to the algebraic decoherence in strongly interacting systems [14].

Phase transitions have been observed in the presence of a particle or energy flow in various spin chains [15]. For example, the equilibrium phase diagram of the transverse field Ising model has two phases: ordered and disordered; while in the presence of particle flow a new phase appears, which carries a nonzero particle flux [16].

The density matrix of the nonequilibrium steady state (NESS) of a noninteracting fermionic system is associated with an effective Hamiltonian [3]. In this formalism, phase transitions can be observed directly from the spectrum of the effective Hamiltonian, which shows features absent in the closed system. For example, a topological phase transition has been found in a cold atomic system subjected to laser irradiation [3].

Equilibrium phase transitions are characterized by discontinuous derivatives of the free energy [17]: the order of the transition is equal to the order of the first discontinuous derivative. In a nonequilibrium situation the free energy is not a well-defined statistical quantity. The partition function, on the other hand, remains well defined also for a nonequilibrium system, as well as entropy, which is given by the logarithm of the number of microstates [18]. Starting from the partition function or entropy we can define the (nonequilibrium) susceptibilities even though the free energy is ill defined [17]. The susceptibility diverges at the transition point [19]. For the second-order quantum phase transition (QPT) the divergence is physical and detectable, while it is a  $\delta$ -function-like divergence for a first-order transition. This means that in an infinite system undergoing a first-order phase transition, when the divergence equals the Dirac  $\delta$  function, we can only observe the step (discontinuity) in susceptibility, while the (infinitely narrow) Dirac  $\delta$  peak is not measurable.

**A. Short overview**

In this paper we study the fermionic chain connected to the memoryless bath at every site of the chain, hence we consider the Lindblad equation for noninteracting fermions [5,20–22]. The ends of the chain are connected to noninteracting memoryless leads [22,23]. The difference in chemical potential induces the particle flow in the system. We find a first-order QPT that separates the regimes of coherent and dissipative transport along the chain. The coherent state is characterized by the

constant current along the chain, while in the dissipative state the current induced by the coupling to the reservoirs decays exponentially inside the chain. QPT between the two happens already at an infinitesimally small coupling to the environment, i.e., the critical coupling value is zero. The transition can be understood microscopically from the fact that the density matrix is decomposed into the tensor product of one-site density matrices in the bulk. The phenomenological reason for the transition is breaking of the time-reversal symmetry by the dissipation along the chain. From the thermodynamic point of view, the transition is a consequence of the entropy-per-site jump. The bulk susceptibility also has a jump at the transition. These facts make us conclude that it is a first-order phase transition. We also detect the jump of the steady-state current at the ends of the chain for sufficiently long chains. We can observe this nonequilibrium QPT in the spectrum of the effective Hamiltonian of the NESS: the gap present for zero dissipation along the chain closes in the presence of dissipation. A nonequilibrium QPT in the system coupled to the Markovian bath has also been observed in the  $XY$ -spin chain [2,5] and in the  $XX$ -spin chain [1].

The phase transitions are normally considered in the thermodynamic limit and the effects of the boundaries (finite-size effects) are neglected (or, in numerical work, systematically eliminated, e.g., by finite-size scaling). When we discuss the transition between the coherent transport through the chain and decoherent state induced by dissipation, we cannot neglect the effects of the boundaries, because the particle current is due to the injection of particles at the ends of the chain. Therefore, we study the particle-particle correlation functions and the electrical susceptibility in the NESS at the ends of the chain and observe power-law divergences as a function of dissipation strength along the chain.

We also consider the workings of dissipation in the presence of disorder. We find that any memoryless dissipation extended along the chain destroys the localization by disorder. This result supports previous studies by the scattering matrix approach [24] and the Landauer-type approach with decoherence [25]. The phase transition to the dissipative state is universal and preserved in the presence of disorder.

## II. MODEL AND FORMALISM

We are interested in the properties of the nonequilibrium steady state of a chain of noninteracting fermions linearly coupled to several noninteracting fermionic baths (reservoirs; we use the two terms as synonymous). The full Hamiltonian of such system is

$$H_{\text{full}} = H_{\text{sys}} + \sum_{i,\alpha} H_{i,\alpha,\text{coup}} + \sum_{i,\alpha} H_{i,\alpha,\text{bath}}, \quad (1)$$

where  $H_{\text{sys}}$  is the tight-binding Hamiltonian of the system:

$$H_{\text{sys}} = \sum_{\{ij\}} t_{ij}(a_i^\dagger a_j + \text{H.c.}) + \sum_i U_i a_i^\dagger a_i, \quad (2)$$

with  $\{ij\}$  denoting the links between the sites,  $t_{ij}$  is the hopping amplitude between the sites  $i$  and  $j$  and  $U_i$  is an on-site potential. By  $H_{i,\alpha,\text{bath}}$  we denote the Hamiltonian of the bath: the index  $i$  here stands for the site of the chain, while the index

$\alpha$  denotes different baths coupled to the same site:

$$H_{i,\alpha,\text{bath}} = \sum_k \epsilon_{i,\alpha,k} b_{i,\alpha,k}^\dagger b_{i,\alpha,k}. \quad (3)$$

The annihilation operators in the baths are denoted by symbol  $b_{i,\alpha,k}$ , while the annihilation operators in the chain are  $a_i$ . Finally  $H_{i,\alpha,\text{coup}}$  is the coupling between the system and the bath, with the coupling strength  $p_{i,\alpha,k}$ :

$$H_{i,\alpha,\text{coup}} = \sum_k p_{i,\alpha,k} (b_{i,\alpha,k}^\dagger a_{i,\alpha} + \text{H.c.}). \quad (4)$$

In our model we have exactly two baths at every site which we can denote as “incoming” and “outgoing”, with  $\alpha \in \{(i),(o)\}$ . The baths are described by the spectral function:

$$J_{i,\alpha}(\omega) = \sum_k |p_{i,\alpha,k}|^2 \delta(\omega - \epsilon_{i,\alpha,k}). \quad (5)$$

For a noninteracting system it has been shown [11,26] that under the assumption of constant spectral density in the reservoirs

$$J_{i,\alpha}(\omega) = v_{i,\alpha}$$

and for the plus/minus infinite chemical potential in the reservoirs the time evolution of the system is described by the Lindblad equation:

$$\begin{aligned} i \frac{d\rho}{d\tau} &= \mathcal{L}\rho, \mathcal{L}\rho \\ &= [H, \rho] + i \sum_{j,i/o} \{2\ell_j^{(i/o)} \rho \ell_j^{\dagger(i/o)} - [\ell_j^{\dagger(i/o)} \ell_j^{(i/o)}, \rho]\}, \end{aligned} \quad (6)$$

where the operator  $\mathcal{L}$  is called the Liouvillian and  $\ell_j$  are the Lindblad operators responsible for the coupling to the bath:

$$\ell_j^{(i)} = \sqrt{\Gamma_j^{(i)}} a_j^\dagger, \quad \ell_j^{(o)} = \sqrt{\Gamma_j^{(o)}} a_j, \quad (7)$$

$$\Gamma_j^{(i)} = \pi v_{j,+\infty} \sum_k |p_{i,+\infty,k}|^2, \quad \Gamma_j^{(o)} = \pi v_{j,-\infty} \sum_k |p_{i,-\infty,k}|^2, \quad (8)$$

with  $v_{j,\pm\infty}$  being the density of states in reservoirs connected to the site  $j$  with plus/minus infinite chemical potential. The infinite chemical potential ensures Markovian dynamics in the bath [27]: in the reservoir at the chemical potential  $+\infty$  there are always particles which can hop into the system and in the reservoir at the chemical potential  $-\infty$  there is always room for new particles hopping out of the system, therefore such baths are memoryless. The finite bandwidth, finite chemical potential, and finite temperature of the reservoirs would make the evolution equation for the density matrix nonlocal in time [11,26].<sup>1</sup> Let us also note that the coefficients  $\Gamma$  are not necessarily small, they can have any value. The difference from the ordinary derivation [13] is that here both

<sup>1</sup>In the above derivation we have not discussed temperature, as it does not matter in the case of infinite chemical potential. When the chemical potential in the reservoirs becomes finite, the temperature appears as an additional parameter.

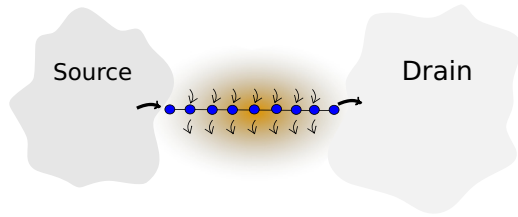


FIG. 1. (Color online) The setup of the problem: one-dimensional chain is connected to the source and the drain as in transport experiments. Every site of the chain is coupled to the environment, which models the dissipation from the leakage of the current due to imperfect insulation. The environment consists of two reservoirs at plus/minus infinite chemical potentials coupled at each site of the chain.

the system and the baths are noninteracting, therefore fewer assumptions are required to get the Lindblad form of the evolution equation.

Let us now apply the Lindblad formalism to our model. Our chain is  $L$  sites long and it is coupled to the source and the drain at infinite bias voltage at its ends:

$$\begin{aligned} \ell_1^{(i)} &= \sqrt{\Gamma^{(i)}} a_1^\dagger, & \ell_1^{(o)} &= 0, \\ \ell_L^{(i)} &= 0, & \ell_L^{(o)} &= \sqrt{\Gamma^{(i)}} a_L. \end{aligned}$$

There is also a dissipation along the chain into a finite temperature bath, which is represented by sources  $\ell_\mu^{(i)} = \sqrt{d\Gamma_\mu^{(i)}} a_\mu^\dagger$  and drains  $\ell_\mu^{(o)} = \sqrt{d\Gamma_\mu^{(o)}} a_\mu$ , for  $\mu = 2, \dots, L-1$ . The  $d\Gamma$  values are not infinitesimal: they are typically much smaller than  $\Gamma^{(i,o)}$  but can take any value in principle; the notation  $d\Gamma$  is just for convenience. Schematically, the dissipative wire setup we study is depicted in Fig. 1. From now on in the text and in the plots the  $\Gamma_\mu$  values are measured in the units of the hopping  $t$ , which we assume to be constant along the chain (in other words we put  $t_{ij} = t = 1$ ).

### A. Solving the Lindblad equation

The solution of the Lindblad equations for noninteracting fermions is notably simplified in the superfermionic representation [21,22], which is based on the doubling of the degrees of freedom as in thermofield theory. Here instead of solving a differential equation for the evolution of the  $2^L \times 2^L$  density matrix, the calculations are done with the  $2L \times 2L$  matrices. The observables of the NESS are computed directly. What is more, the full-counting statistics of the transport through the ends of the chain can be obtained by introducing the counting field, which yields the generating function of the counting statistics [22,23]. We will present the results for the first cumulant of the generating function, i.e., the current, as well as for the ratio between the second and the first cumulant, which characterizes the noise in the system and is called the Fano factor.

We evaluate the current along the chain by averaging the local current operator over the NESS:

$$\hat{j}_k = -it(a_k^\dagger a_{k+1} - a_{k+1}^\dagger a_k). \quad (9)$$

At the ends of the chain the current and the Fano factor are given by the derivatives of the generating function.

The Liouvillian for noninteracting fermions in the superfermionic representation becomes quadratic after performing the particle-hole transformation [22], as the Liouvillian becomes diagonal in the basis  $\{f, f^\dagger, \tilde{f}, \tilde{f}^\dagger\}$ , see Appendix. The density matrix of the NESS is a vacuum for the operators  $f$  and  $\tilde{f}$  (see Appendix). As there exists a linear relation between the initial basis  $\{a, a^\dagger, \tilde{a}, \tilde{a}^\dagger\}$  and the basis  $\{f, f^\dagger, \tilde{f}, \tilde{f}^\dagger\}$ , the density matrix of the NESS is quadratic:

$$\rho_{\text{NESS}} = \frac{\exp(\mathcal{H}_{mn} a^\dagger \tilde{a}^\dagger) |00\rangle_{a\tilde{a}}}{\langle I | \exp(\mathcal{H}_{mn} a^\dagger \tilde{a}^\dagger) |00\rangle_{a\tilde{a}}}, \quad \mathcal{H}_{jn} = \tilde{\kappa}_{ni}^{-1} \kappa_{ji}, \quad (10)$$

where the matrix  $\kappa$  is connected to the matrix of the eigenvectors  $P$  of the transformation which diagonalizes the particle-hole transformed Liouvillian [22] (see Appendix), namely  $T = P^{-1}$ ,  $\kappa_{kj} = T_{kj}$  and  $\tilde{\kappa}_{kj} = T_{k+L,j}$  for  $k, j = 1, \dots, L$ . Notice that  $i\mathcal{H}$  is a Hermitian matrix as  $\rho$  is Hermitian, and  $\langle I |$  is the left vacuum,  $|I\rangle = \sum_n |nn\rangle_{a\tilde{a}}$  [21], where by  $n$  we denote the state in the  $a$  basis. Therefore,  $i\mathcal{H}$  can be considered as an effective Hamiltonian of the NESS.

## III. DISSIPATION-INDUCED PHASE TRANSITION

In this section we first observe the dissipation-induced phase transition in the transport properties at the ends of the chain and in the bulk and then we characterize the transition in the thermodynamic limit. Afterwards we discuss some specific aspects of the transition at the ends of the chain by studying the response to electric field and the particle-particle correlation functions close to the ends and reveal its microscopic nature. Finally, we study the influence of the dissipation on the phenomenon of delocalization in disordered systems.

### A. Observation of the transition

We model dissipation along the chain as tunneling to the metallic gate in the absence of good isolation of the one-dimensional chain from the environment. To implement this we couple a source and a sink to every site of the chain [21]. We also allow for disorder in the hybridization strengths  $d\Gamma_\mu^{(i/o)}$  to account for different tunneling rates to the environment.

The fermionic chain coupled to the reservoirs only at its ends has a uniform current along its length due to particle conservation. Let us call the state of such a system coherent as the current at its ends depends on both couplings. On the other hand we call the state of the system decoherent when the current through a given end depends only on the coupling of the reservoir at this end.

We only expect to find a phase transition and the associated discontinuities in the thermodynamic limit, i.e., in an infinite system. For that reason we start by looking at a chain long enough that there is no dependence on its length, Fig. 2(b). We see a jump both in the current and in the Fano factor when the dissipation is switched on, Fig. 2(a). Reference [23] provides the large deviation calculation for the current distribution function of the chain coupled to the reservoirs only at its ends. The current distribution is discontinuous as a function of the couplings to the reservoirs and the author suggests that this is the reason of the phase transition also for the system dissipative along its length.

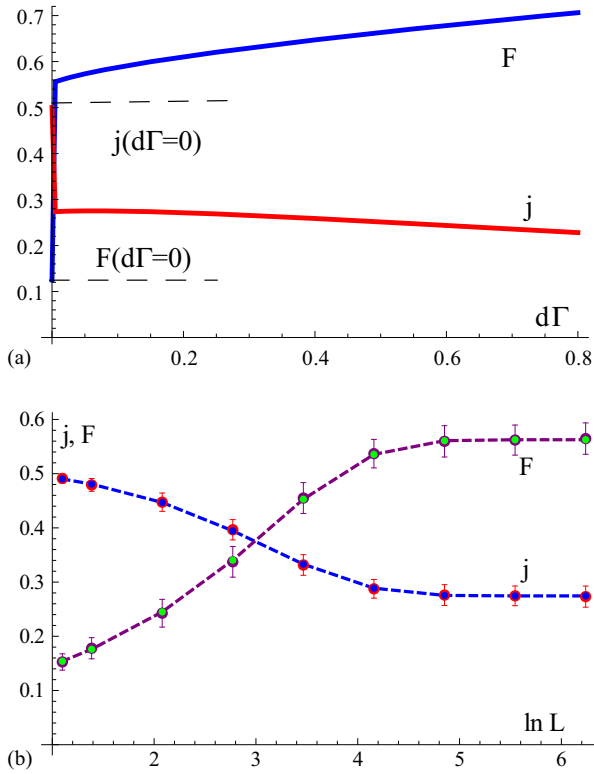


FIG. 2. (Color online) (a) The jump of the current,  $j$ , and the Fano factor,  $F$ , at infinitesimally small dissipation constant along the chain  $d\Gamma = d\Gamma^{(i)} = d\Gamma^{(o)}$  ( $\Gamma^{(i)} = \Gamma^{(o)} = 1$ ). (b) Dependence of the current  $j$  and the Fano factor  $F$  through the ends of the chain on the length  $L$  for random dissipation along the chain taken from the range  $d\Gamma^{(i)}, d\Gamma^{(o)} \in (0, 0.04)$  (points with error bars) and for the constant dissipation with the strength  $d\Gamma^{(i)} = d\Gamma^{(o)} = 0.02$  (points and the dashed lines). Here and everywhere else in the text and the plots the  $\Gamma_\mu$  values are measured in the units of the hopping  $t$ .

In order to understand better the nature of the states on both sides of the transition, let us consider the current along the chain. We compute the expectation value of the local current operator (9) in the NESS for every link of the chain. For a nondissipative system it is constant along the chain due to the current conservation. For the dissipative case it decays exponentially inside the system, Fig. 3. One would certainly expect such behavior in the presence of the drains only. But in our setup we have both the source and the drain attached to every site of the chain. Therefore, we conclude that the exponential decrease of the current is connected to the coherence losses due to coupling to the memoryless environment, and not simply to the current leakage into the drains.

If we allow for a random distribution of the dissipation along the chain, the current averaged over disorder configurations decays with the same exponent as the current in the system with uniform dissipation, with the magnitude equal to the mean of the distribution of the disordered couplings, Fig. 3.

With increasing dissipation strength, the current through one end of the chain becomes only weakly dependent on the coupling at the other end of the chain because the coherence of the transport through the chain is lost upon adding the

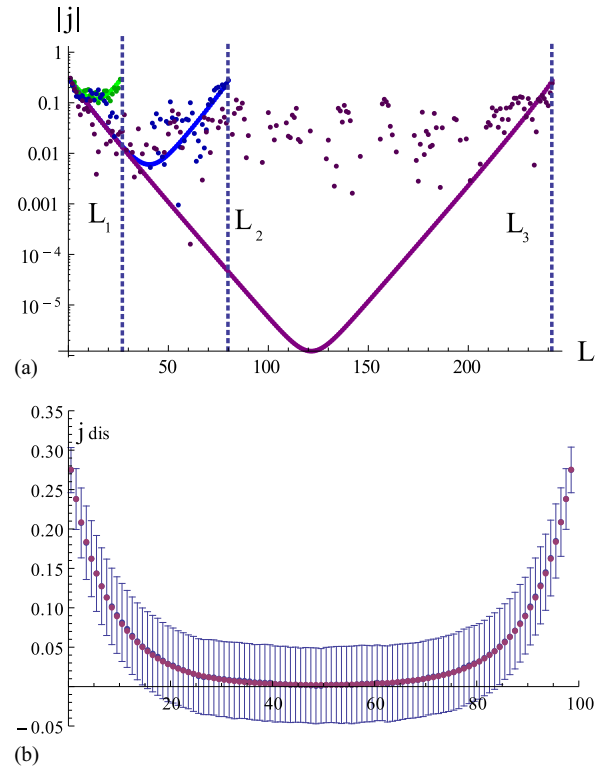


FIG. 3. (Color online) Exponential decay of the current along the chain. (a) Logarithmic scale, different lengths of the system. The currents in the system without randomness in dissipation are represented by the regular sets of points (forming solid lines). Darker, irregularly scattered points represent the current for one realization of the disorder in dissipation along the chain. (b) The current through a dissipative chain after averaging over different disorder realizations. The scale is linear (not logarithmic) to show the standard deviation of the (fluctuating, random) current. Notice that the negative values of the current are physical, because some realization of the (random) couplings  $d\Gamma$  can give an overall current flowing in the opposite direction. The couplings at the ends of the chain are  $\Gamma^{(i)} = \Gamma^{(o)} = 1$ ,  $d\Gamma = 0.05$ . For the average over disorder  $d\Gamma_j^{(i)}, d\Gamma_j^{(o)} \in (0, 0.1)$ ,  $j \in (2, L - 1)$ .

dissipation along the chain, Fig. 4. Here we make a plot for the constant dissipation rate along the chain since the current averaged over disorder in coupling strengths is the same as in the case of the constant dissipation (see Fig. 3).

Both the presence of the jump in the transport characteristics at the ends of the chain and the coherence/decoherence transition in the current along the chain suggest that any nonzero dissipation along the chain induces the QPT. It is not a van der Waals-type transition, meaning there is no analog of the latent heat, that is, excitation of internal degrees of freedom, but the extra energy is instead exchanged with the bath.

### 1. Classical analogue

The Lindblad approximation for the driving at the ends of the chain and decoherence along the chain make our quantum model less quantum and more classical. This is exemplified by comparing our results with a classical model introduced

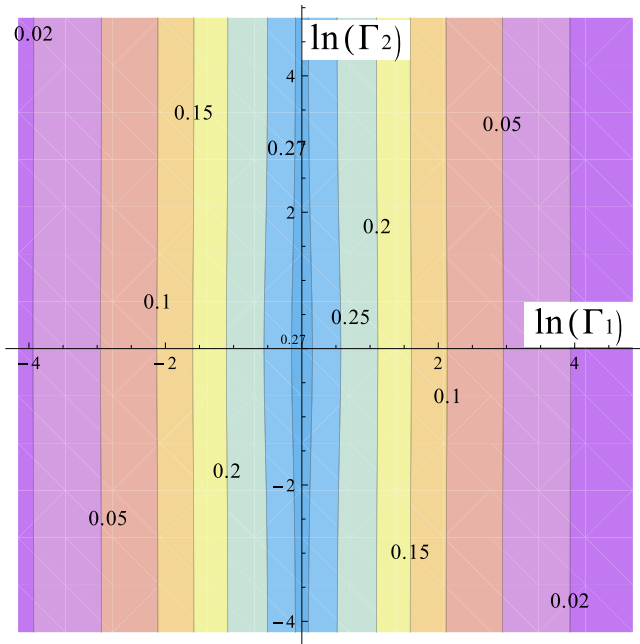


FIG. 4. (Color online) Logarithmic plot of the current flowing from the system into the reservoir at the beginning of the chain (denoted by 1) as a function of the hopping rates at the ends of the chain, in the presence of the constant dissipation along the chain,  $d\Gamma^{(i)} = d\Gamma^{(o)} = 0.02$ . Increasing the dissipation makes the current through one end independent of the coupling at the other end of the chain. In this plot we denote  $\Gamma^{(i)} = \Gamma_1$ ,  $\Gamma^{(o)} = \Gamma_2$ .

by Roche, Derrida, and Doucot [28] for studying the classical version of the Landauer picture of a quantum conductor, where we also observe the exponential decay of the current inside the chain as well as the jump of the steady-state current at the ends of the chain upon introducing the dissipation along the chain.

We consider a counterflow model [28]: the system is modeled by an  $L$ -site chain, where each of the sites may contain two particles, one right-moving and one left-moving. It is analogous to the quantum scattering problem. Let us call the walls between the sites tunnel barriers. The time is discrete. At each time step the right-moving state on the left of the barrier and the left-moving state on the right of the barrier are transferred to the right-moving state on the right of the barrier and the left-moving state on the left of the barrier, respectively:

$$(0_{r,k-1}, 0_{l,k}) \rightarrow (0_{r,k}, 0_{l,k-1}), \quad (11)$$

$$(1_{r,k-1}, 1_{l,k}) \rightarrow (1_{r,k}, 1_{l,k-1}), \quad (12)$$

$$(0_{r,k-1}, 1_{l,k}) \rightarrow \begin{cases} (0_{r,k}, 1_{l,k-1}) \text{ with prob. } T, \\ (1_{r,k}, 0_{l,k-1}) \text{ with prob. } (1 - T) \end{cases} \quad (13)$$

$$(1_{r,k-1}, 0_{l,k}) \rightarrow \begin{cases} (1_{r,k}, 0_{l,k-1}) \text{ with prob. } T, \\ (0_{r,k}, 1_{l,k-1}) \text{ with prob. } (1 - T), \end{cases} \quad (14)$$

where on the left-hand/right-hand side of the arrow is the state before/after the time step respectively, 0 and 1 denote the state of the system (empty/full), the subscripts  $r/l$  stand for right-/left-moving and  $k$  stands for the cell number. The first and the last cell are updated at every time step to account for

the contact with the reservoirs:

$$(1_{r,1}, 0_{l,1}) \quad \text{with prob. } \rho_R, \quad (15)$$

$$(0_{r,1}, 0_{l,1}) \quad \text{with prob. } (1 - \rho_R), \quad (16)$$

$$(0_{r,L}, 1_{l,L}) \quad \text{with prob. } \rho_L, \quad (17)$$

$$(1_{r,L}, 1_{l,L}) \quad \text{with prob. } (1 - \rho_L). \quad (18)$$

The configuration space of this process grows exponentially with the the number of sites: it contains  $2^L$  configurations. This makes it complicated to calculate the counting statistics using the transition matrix approach [28]. In general, the described model has a diffusive behavior: the current through the system decreases with increasing system size [28] (this happens because each transmission process is a stochastic process). In our model we obtain pure ballistic behavior by moving all particles in the middle of the chain (which are independent of the dynamics on the first and the last site) as a whole, which is just what ballistic propagation means.

While earlier work [28] considers only the flux of particles at the end of the chain, we introduce the dissipation in the middle of the chain as a classical analog of decoherence (from now on we call it decoherence to emphasize the lack of true quantum-mechanical coherence in the classical model) as a spontaneous appearance/disappearance of right/left moving particles in between two propagation steps. Therefore, our algorithm of time evolution of the dissipative chain is

(i) Initialize the time step:

(a) generate an arbitrary initial state in the first step;

(b) in the subsequent steps: update first the occupation on the first and the last site of the chain according to (15)–(18). Then update the occupation number in the middle, which changes due to decoherence: if both left- and right-moving states at the site  $k$  are empty, then with probability  $d\Gamma^{(i)}/2$  one of them becomes occupied. If only the left- or right-moving state is empty, then this state becomes full with probability  $d\Gamma^{(i)}$ . The analogous update is done for hopping out of the chain with the rate  $d\Gamma^{(o)}$ .

(ii) Move the particles:

(a) the right/left movers on the site from 2 to  $(L - 2)/3$  to  $L - 1$  from are shifted in the ballistic way (the particle is moved by one site, if the site with the corresponding chirality on its way is empty);

(b) make a move of the states around the barriers according to rules (11)–(14);

(c) shift particles close to the ends if more ballistic motion is possible with respect to the configuration after (11)–(14) comparing to the initial configuration.

(iii) Repeat the steps (i) and (ii).

According to our numerical simulation the average over the time evolution of a single state equals to the average over different initial states evolved for a fixed time, which is long enough to approach the steady state, as we would expect in an ergodic system. We present the long-time averages over time of the evolution of a single state as it is less computationally consuming comparing to the other averaging procedure.

The current through the chain can be determined in two ways: as the difference between the right and left movers at each cell or as the number of the particle transmissions between

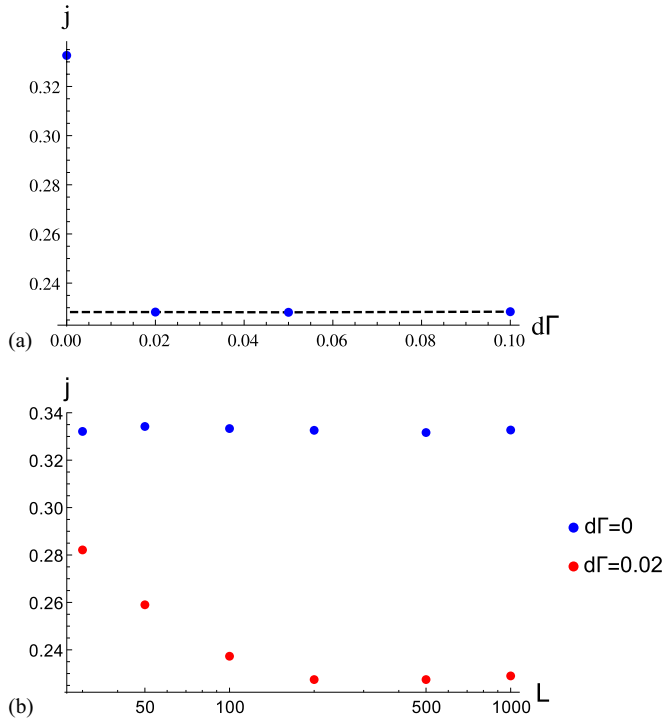


FIG. 5. (Color online) (a) The jump of the current at the end of the chain upon switching on the decoherence along the chain in the classical counterflow model. (b) Dependence of the current through the first site of the chain on the length of the chain. Compare to Fig. 3, where analogous behavior is observed for the quantum chain modeled by the Lindblad equation.  $\Gamma_1^{(in)} = \Gamma_2^{(out)} = 0.5$

the neighboring cells. Qualitatively these approaches give the same answer for our decoherent problem.

To compare our numerical simulation with the Lindblad approach we fix  $\rho_R = 1$  and  $\rho_L = 0$  to model the leads at plus/minus infinite voltage. The time-averaged current decays exponentially from the ends of the chain toward the middle, Fig. 6. The saturation of the exponential decay in the middle happens due to finite time of averaging. The average current

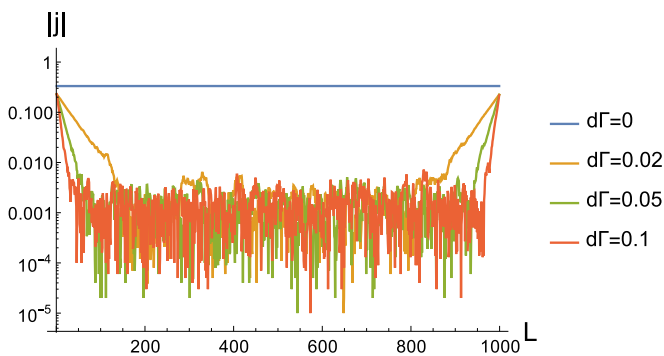


FIG. 6. (Color online) The dependence of the current on the site index for different decoherence rates  $d\Gamma$  in logarithmic scale in the classical counterflow model: the exponential decay of the current from the ends toward the middle of the chain is clearly visible, suggesting a similar mechanism of decoherence as in the quantum chain in Fig. 4.  $\Gamma_1^{(in)} = \Gamma_2^{(out)} = 0.5$ ,  $t_{max} = 10^5$ .

through the end of the chain jumps when decoherence is introduced in the system, Fig. 5. To observe the clear jump the number of time steps should be large enough that the system forgets about its initial configuration, at least about  $L/d\Gamma$ .

The behavior of the quantum chain is thus qualitatively reproduced by the classical stochastic model. It might therefore seem that the term quantum phase transition we have used for the transition in the quantum chain is a misnomer. This is not the case, since the classical counterflow model is stochastic and thus exhibits fluctuations around the expectation values, i.e., averaged values. The generating function of the counterflow model is thus analogous to the action of a quantum system, and the jump of the suitably defined classical current is formally analogous to the QPT observed earlier. A truly classical system (with no fluctuations) would not show such a phase transition.

## B. First-order phase transition in the thermodynamic limit

Phase transitions are normally studied using the thermodynamic quantities and the response functions. In a nonequilibrium situation the partition function and the entropy are well-defined thermodynamic quantities. Here we concentrate on the entropy and the response to the electric field, and eventually explain the microscopic nature of the transition.

### 1. Entropy

The NESS is Gaussian, Eq. (10), as it can be represented as an exponent of a quadratic operator. Therefore, its effective Hamiltonian is a Hamiltonian of noninteracting fermions. In analogy with equilibrium statistical physics one can connect the entropy of the NESS to the eigenvalues  $\mu_i$  of the effective Hamiltonian (10) [29]:

$$S = - \sum_i \left( \ln(1 + e^{-\epsilon_i}) + \frac{\epsilon_i}{1 + e^{\epsilon_i}} \right), \quad \mu_i = e^{-\epsilon_i}. \quad (19)$$

The entropy per unit length  $S = S/L$  does not depend on the system length for sufficiently long systems and experiences a jump upon turning on the dissipation along the chain, Fig. 7. For a chain without dissipation the specific entropy always depends on the couplings to the reservoirs at the ends of the chain, while for a dissipative system it does not depend on the couplings to the leads in the thermodynamic limit (the contribution from the boundaries is of the order of  $1/L$ ). The specific entropy tends to a value depending only on the ratio of the incoming and outgoing rates along the chain  $\gamma = d\Gamma^{(i)}/d\Gamma^{(o)}$ :

$$S = \ln(1 + \gamma) - \frac{\gamma}{1 + \gamma} \ln \gamma. \quad (20)$$

This corresponds to the entropy of the single site coupled to only two baths by the Lindblad operators  $\sqrt{d\Gamma^{(i)}}a^\dagger$  and  $\sqrt{d\Gamma^{(o)}}a$ . Indeed, the reduced density matrix of a site in the middle of the chain is the same as for a single site coupled to two baths up to a factor exponentially small in  $L$ . The coupling to the rest of the chain is irrelevant. The current in the middle of the chain vanishes, but what is happening is even stronger: the correlation between two neighboring sites vanishes exponentially  $\langle c_{i+1}^\dagger c_i \rangle_{\text{NESS}} = O[\exp(-\beta i)]$ , where  $i$  is the number of the site in the middle of the chain and  $\beta$  is the

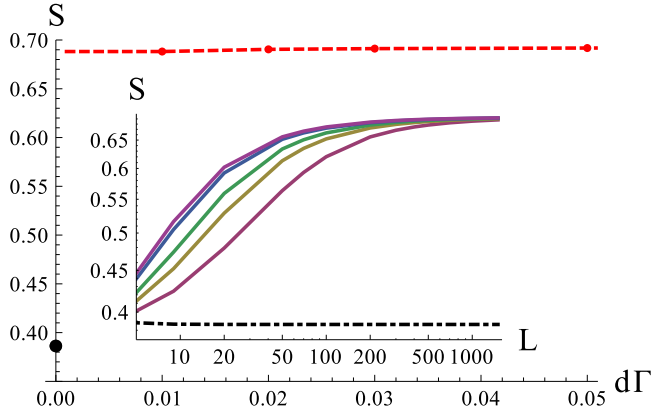


FIG. 7. (Color online) Entropy jump at the transition point as a function of the dissipation strength. The dashed line is in agreement with Eq. (20). Inset: dependence of the entropy on the chain length for different dissipation strengths  $d\Gamma = 0.01, 0.02, 0.03, 0.04, 0.05, 0.06$  (from top to bottom solid curve respectively), the dash-dotted line corresponds to the entropy in the absence of the coupling to the environment, the point at  $d\Gamma = 0$  at the main plot.

slope of the exponential decay. Therefore, we can write down the reduced density matrix of the middle part of the system neglecting the exponentially small correlations between the sites as a tensor product of the density matrix of one site connected to two baths.

## 2. Spatial decoupling in the density matrix

Such a spatial decoupling of a density matrix for a completely translationally invariant system (without current injection/removal at the ends) is evident. We can diagonalize the Liouvillian by the Fourier transform. Indeed, in terms of Ref. [22] the matrix  $M$  after the Fourier transform obtains the block structure:

$$\mathcal{L} = \sum_k (a_k^\dagger \tilde{a}_k) M_k \begin{pmatrix} a_k \\ \tilde{a}_k^\dagger \end{pmatrix} - i \sum_k (d\Gamma^{(i)} + d\Gamma^{(o)}), \quad (21)$$

$$M_k = \begin{pmatrix} -i\delta\Gamma + 2t \cos k & 2d\Gamma^{(o)} \\ -2d\Gamma^{(i)} & i\delta\Gamma + 2t \cos k \end{pmatrix} \quad (22)$$

with  $\delta\Gamma = d\Gamma^{(i)} - d\Gamma^{(o)}$ . Each of the matrices  $M_k$  can be diagonalized:  $M_k = P_k^{-1} D_k P_k$ , where  $D_k$  is a diagonal matrix and  $P_k$  is a matrix of eigenvectors. This transformation determines the basis where the Liouvillian is diagonal:

$$\begin{pmatrix} f_k \\ \tilde{f}_k^\dagger \end{pmatrix} = P \begin{pmatrix} a_k \\ \tilde{a}_k^\dagger \end{pmatrix}, \quad (f_k^\dagger \tilde{f}_k) = (a_k^\dagger \tilde{a}_k) P^{-1}, \quad (23)$$

$$\mathcal{L} = \sum_k (\lambda_k f_k^\dagger f_k - \lambda_k^* \tilde{f}_k^\dagger \tilde{f}_k). \quad (24)$$

Here we assumed that  $D_k = \text{diag}(\lambda_k, \lambda_k^*)$  and  $\text{Im}\lambda_k < 0$ . This structure leads to cancellation of the constant term in the Liouvillian.

The steady state density matrix is determined as the vacuum of operators  $f_k$  and  $\tilde{f}_k$ . The transformation to the basis of the

$a, a^\dagger$  occupation numbers gives the density matrix:

$$\rho = \sum_k \frac{\exp(\mathcal{H} a_k^\dagger \tilde{a}_k^\dagger) |00\rangle_{a_k \tilde{a}_k}}{a_k \tilde{a}_k \langle I | \exp(\mathcal{H} a_k^\dagger \tilde{a}_k^\dagger) |00\rangle_{a_k \tilde{a}_k}}, \quad (25)$$

$$\mathcal{H} = i \frac{d\Gamma^{(i)}}{d\Gamma^{(o)}}, \quad |I\rangle_{a_k \tilde{a}_k} = |00\rangle + |11\rangle. \quad (26)$$

The effective Hamiltonian  $\mathcal{H}$  is a constant, therefore the Fourier transform gives the density matrix which is a tensor product in position space:

$$\rho = \otimes_i \left( \frac{d\Gamma^{(o)}}{d\Gamma^{(o)} + d\Gamma^{(i)}} |00\rangle_{a_i \tilde{a}_i} + \frac{d\Gamma^{(i)}}{d\Gamma^{(o)} + d\Gamma^{(i)}} |11\rangle_{a_i \tilde{a}_i} \right). \quad (27)$$

We can thus conclude that the density matrix is local in space. For the case of disordered leakage along the chain one cannot perform the Fourier transform of the Liouvillian analytically but numerical calculation shows that the density matrix averaged over disorder is again represented by the tensor product of single-site density matrices. For a single realization of the disorder in the couplings along the chain the decomposition is not exact, as shown in Fig. 3(a) for the current through the chain for a single realization of the disorder.

## 3. Response to the electric field

The response functions are good indicators of the equilibrium phase transitions. Let us consider a response of the current to a constant electric field  $E$  applied along the chain. In the tight-binding model it is incorporated as a linearly growing on-site potential:  $U_m = mEl_0$ , where  $l_0$  is the lattice constant. In most models of the transport one assumes that the current flow is due to an electric field applied along the system. Here we have a current through the chain due to the coupling to the reservoirs. The difference in on-site potential from site to site can be viewed as applying an additional field along the chain. For example, in a cold atom system one can imagine a lattice constructed with varying depths of the potential well. In the decoherent phase, the electric field changes the response function only locally: close to the ends we expect the susceptibility to be different from the middle of the system due to the presence of coherence because of the coupling to the reservoirs. The linear response of the current to the electric field applied along the chain vanishes, and only the quadratic part is left, Fig. 8, inset:

$$j_{\text{NESS}}(E, d\Gamma^{(i)}, d\Gamma^{(o)}; L) - j_{\text{NESS}}(0, d\Gamma^{(i)}, d\Gamma^{(o)}; L) = \sigma(d\Gamma^{(i)}, d\Gamma^{(o)}; L) E^2. \quad (28)$$

Here we also notice that there is a scaling with  $E$ : the dependence of the conductivity on length scales with  $E^2$  for the same dissipation rates along the chain  $d\Gamma^{(i)}, d\Gamma^{(o)}$ . We attribute the quadratic dependence on  $E$  to the structure of the NESS. The Ohm's law is an outcome of the linear response theory, which implies that the current is a consequence of the electric field applied to the equilibrium system. In our case the situation is tremendously different—from the physical point of view, the current is already present in the system due to contact with the leads even before applying the electric field along the system. From the viewpoint of the response theory, the response is considered with respect to the nonequilibrium steady state. It

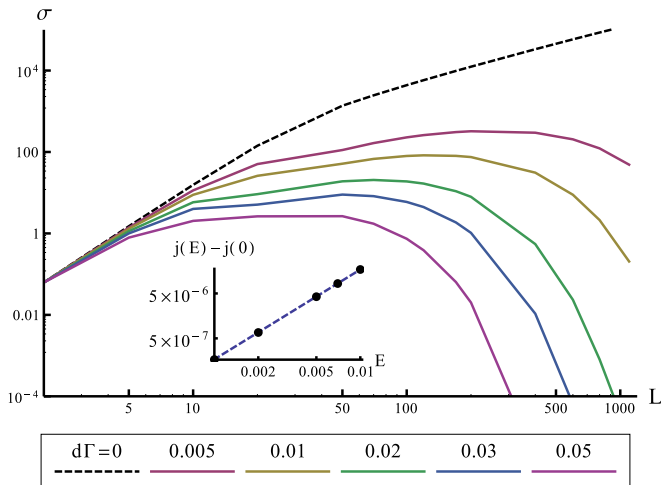


FIG. 8. (Color online) Main plot: the convergence of the nonlinear response to the electric field for long systems in the bulk of the chain. Solid lines correspond to different coupling strength  $d\Gamma = 0.005, 0.01, 0.02, 0.03, 0.05$  (from top to bottom) and the dashed line is  $d\Gamma = 0$ . Inset: quadratic scaling of  $j(E) - j(0)$  with the applied electric field (the scale in logarithmic).

is thus possible that the linear part of the response vanishes and only the nonlinear part is present.

The nonlinear response to the electric field vanishes in the bulk of the chain, Fig. 8. The response in the nondissipative system grows infinitely in the thermodynamic limit because of the translational invariance in the bulk. Indeed, when we make the hopping parameters disordered (i.e., make them vary along the chain), the infinite growth of  $\sigma$  is suppressed. Therefore, there is a discontinuity in the value of  $\sigma$  for infinitesimally small  $d\Gamma$ . It is consistent with the first-order phase transition.

### C. Near-boundary effects

The symmetrized particle-particle correlation function:

$$C_i(k) = \langle a_{i+k}^\dagger a_i + a_i^\dagger a_{i+k} \rangle_{\text{NESS}} \quad (29)$$

provides further information about the transition. The correlations at the ends of the system are present and they decay exponentially:  $C_i(k) \propto \exp(-k/\xi_i)$ ,  $i \sim 1$  or  $i \sim L$ , where  $\xi$  is a correlation length, Fig. 11. We find the power-law divergence of the correlation length as the function of dissipation at zero dissipation rate along the chain. Inside infinitely long systems the correlations vanish:  $\xi_i \rightarrow 0$ ,  $i \sim L/2$ ,  $L \rightarrow \infty$ , as all coherence in the system is lost.

The nonlinear conductivity converges to a nonzero value at the boundaries of the chain, Fig. 9, unlike in the bulk of the chain, where it converges to zero. This happens due to some remaining coherence at the ends of the chain. Even more, there is a power-law scaling of the conductivity with dissipation strength, the parameter, which drives the phase transition, inset of Fig. 9.

To further corroborate the finding of the continuous QPT at the edges, let us now consider the spectrum of the effective Hamiltonian,  $\mathcal{H}$ . For the translationally invariant dissipative system from Sec. III B 2 the spectrum of the effective Hamiltonian is a  $\delta$  function  $\delta(\epsilon - \text{const} \times d\Gamma^{(i)}/d\Gamma^{(o)})$ ,

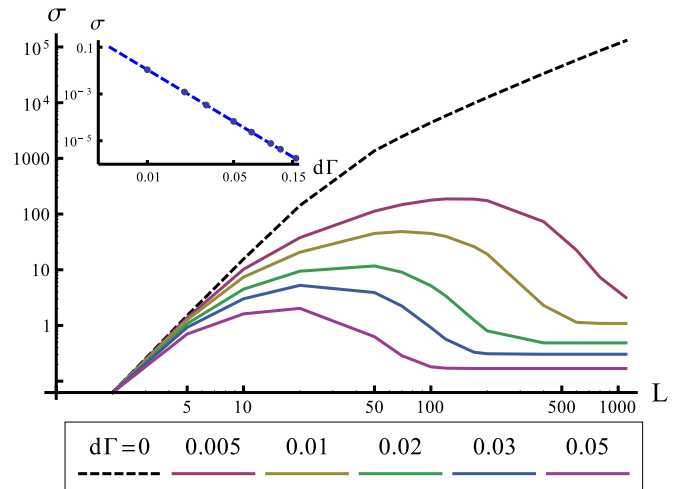


FIG. 9. (Color online) Main plot: the convergence of the nonlinear response to the electric field for long systems at the ends of the chain. Solid lines correspond to different coupling strength  $d\Gamma = 0.005, 0.01, 0.02, 0.03, 0.05$  (from top to bottom) and the dashed line is  $d\Gamma = 0$ . Notice that the nonlinear conductivity at the ends points stays nonzero also in the thermodynamic limit. As in Fig. 8, the conductivity is infinite in the absence of dissipation. Inset: scaling of  $\sigma$  with disorder strength with power-law fit:  $\sigma = \alpha d\Gamma^\beta$ ,  $\beta = 3.161 \pm 0.001$ .

where the constant comes from the freedom of choice of the effective Hamiltonian, which is connected to the freedom of choice of constants in front of the left and the right vacuum of the Liouvillian. When we take into account the whole chain with the end sites, the spectrum of the effective Hamiltonian is influenced by the presence of the ends of the chain: in the absence of the dissipation along the chain the lowest eigenvalue  $\lambda_{\min}$  of  $\mathcal{H}$  is 0, while in the presence of the dissipation  $\lambda_{\min}$  shifts to a nonzero value, Fig. 10. There is a power-law scaling of  $\lambda_{\min}$  with the strength of the dissipation, Fig. 10(b).

### D. Disordered dissipative system

Let us consider a disordered system with random on-site potential  $U_i$  in the Hamiltonian (2). The values  $U_i$  are taken from the uniform distribution with the range  $(0, dU)$ .

It is known that in one spatial dimension disorder always localizes the conservative system [30]. This is the well-known Anderson localization: it happens because the electron waves always interfere so that the overall wave function is localized on the impurities. Such a system is an insulator as the overlap of the electron wave functions at different positions in the chain is exponentially small. This reasoning suggests the scaling hypothesis, which proposes that the conductivity in a disordered system should decrease exponentially with the system size, when the system is in the localized regime.

However, the presence of dissipation changes this: dissipation delocalizes the disordered system, as the dissipation breaks the interference, which is responsible for the localization. For averaging over disorder we used only 15 disorder configurations, as the uncertainties of the average are already small enough in that case (the error bars in the figure are of the size of the symbols in the plot). This happens because

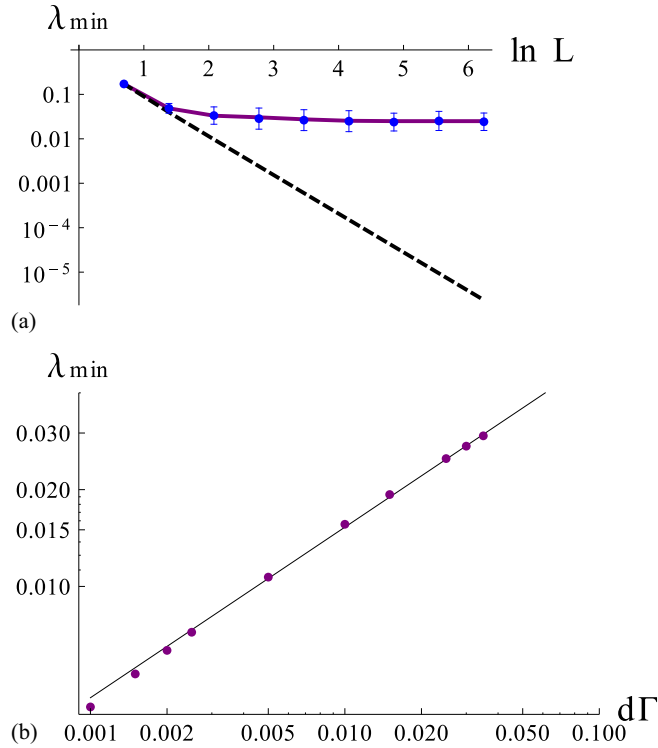


FIG. 10. (Color online) (a) The lowest eigenvalue  $\lambda_{\min}$  of the effective Hamiltonian (10) as a function of the system size for the system without (black dashed line) and with dissipation (blue points: averages over the disorder from the range  $(0, d\Gamma)$ , purple line: constant dissipation with  $d\Gamma/2$ ,  $d\Gamma = 0.025$ ). (b) The scaling of the lowest eigenvalue with disorder strength,  $\lambda_{\min}(d\Gamma)$ , and the power-law fit  $\lambda_{\min} \propto d\Gamma^\beta$  with  $\beta = 0.53 \pm 0.01$ . The couplings to the source and the drain are  $\Gamma^{(i)} = \Gamma^{(o)} = 1$ .

the density matrix of an open quantum system contains the sectors with different particle numbers, hence the values of the current in the NESS can be considered as averaged not only

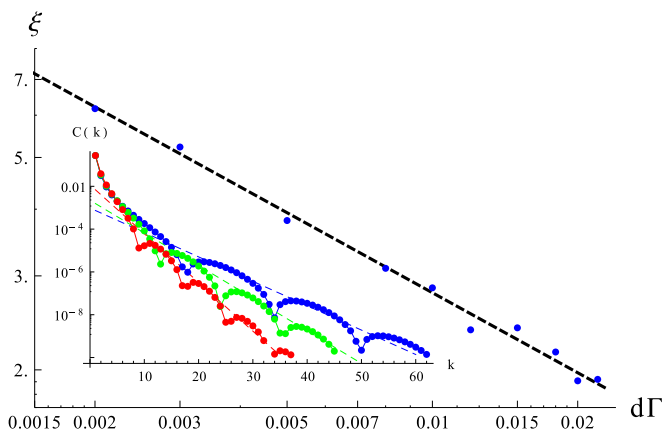


FIG. 11. (Color online) Dependence of the correlation length on the coupling to the environment for  $\Gamma^{(i)} = \Gamma^{(o)} = 1$  (dots) and the power-law fit (dashed line). Inset: correlations at one end of the chain as a function of the position for different couplings strengths  $d\Gamma = 0.005, 0.01, 0.02$  (from top to bottom: blue, green, red) and exponential fits, which determine the correlation length (dashed lines).

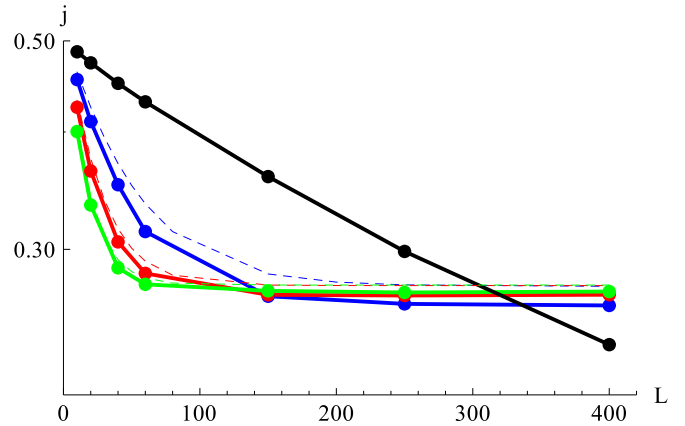


FIG. 12. (Color online) Dependence of the current through a disordered dissipative system on the length of the system for different values of the dissipation along the system,  $d\Gamma = 0, 0.02, 0.03, 0.05$  (from top to bottom at small  $L$ : black, blue, red, green; solid lines:  $dU = 0.3$ , dashed lines:  $dU = 0$ ;  $\Gamma_1 = \Gamma_2 = 1$ ). The current through the system is independent of the system length for a sufficiently long system.

over disorder configurations, but also with respect to different particle numbers.

The general phenomenology of the clean system with dissipation is thus preserved also in the disordered system. The current again reaches a finite (though smaller) value in the thermodynamic limit, and the current at one end only weakly depends on the coupling at the other end. An example is seen in Fig. 12, where for simplicity we consider constant couplings to the environment along the chain and average only over the disorder realizations of the on-site potential.

#### IV. CONCLUSIONS AND DISCUSSION

We have considered the transport properties of a one-dimensional wire with leakage to the environment. In experimental systems, this leakage can happen due to misfabrication and the presence of the tunneling from the wire to a metallic region underneath the wire. We observe a first-order phase transition for infinitely long systems already at infinitesimal dissipation rate along the chain. From the microscopic point of view, this QPT means discontinuous behavior of the density matrix. On the macroscopic level it manifests itself in the jump in the current and the Fano factor. From the thermodynamic point of view we can say that the entropy jumps across the transition. The specific entropy in the dissipative phase is equal to the entropy of a single site coupled to the source and the drain.

Essentially, the phase transition is an anomaly: dissipation breaks the time-reversal invariance [31]. Upon taking the symmetry-breaking parameter (dissipation strength) to zero, we do not recover the result for unbroken symmetry. In the continuum limit it is analogous to the fact that, for example, viscosity effects in a fluid are nonperturbative and the flow undergoes a qualitative change for arbitrarily small nonzero dissipation: the scaling exponents of the correlation functions of the velocities jump at the transition between an ideal and viscous liquid [31]. To understand better the universality of

our finding, we have considered also the classical stochastic counterflow model, which describes a chain with two classes of asymmetric exclusion random walkers, left- and right-moving. In this case, dissipation is modeled by randomly creating or destroying the random walkers with certain probabilities at every (discrete) time step. This model, under suitable assumptions, again shows the same anomaly and the current jumps for arbitrarily small nonzero values of the dissipation. In the counterflow model, the role of quantum fluctuations is taken over by the stochastic fluctuations. In fluid dynamics, the velocity fluctuations make the system effectively quantum. The notion of QPT is thus justified, and the observation of anomaly—breaking of a classical symmetry at the quantum level, i.e., by the loop contributions to the action—becomes natural.

In a different context, the transport theory for dissipative systems has been developed in Refs. [24,32] in the language of the scattering matrices. Our Lindblad-based approach and the scattering approach are different in a few respects. First, let us consider a system without dissipation, coupled to two reservoirs at the ends. The scattering matrix theory describes the case when the wave coming from the reservoir into the system is coherent (just a plane wave), while the Lindblad approach describes the case of incoherent leads—the hopping in the chain happens stochastically. This is also reflected in the transport properties: while for coherent transport the conductivity is proportional to the number of open channels in the system, for the transport induced by incoherent hopping it is not [22]. Now let us move to the dissipative system. In the scattering matrix approach the dissipation is modeled through additional channels, which do not contribute to the transport (for the one-dimensional nondissipative problem the scattering matrix has the format  $2 \times 2$ , for the incoming and the outgoing channel, while in the dissipative case the scattering matrix has a larger dimension, and only two channels describe the transport along the chain whereas the others describe the scattering in the side channels). The dissipation constructed in this way is coherent, while the Lindblad-like dissipation is incoherent.

It is interesting that the spin system coupled to the bosonic bath at every site experiences a second-order phase transition, and only at finite dissipation strength [6–9]. We do not know if the order of the transition is related to the presence or absence of memory or if it is determined by the statistics of the bath.

The phase transition in the quadratic fermionic systems was studied also in Refs. [2,5]. There, the  $XY$  chain coupled to the reservoirs at both ends was considered. The transition manifests itself in the change of behavior of the spin-spin correlation functions and the entanglement entropy, which does not depend on the system size on one side of the transition and grows linearly with the system length on the other side. The authors argue that the transition is of infinite order as all local observables are analytical across the transition. Subsequently the critical behavior has been observed also in the  $XX$ -spin chain [1] coupled to the environment at every site of the chain: the spin-spin correlation functions are short ranged in the nondissipative case, whereas they decay as a power law in the presence of the on-site decoherence. The transition we observe is significantly different from the previously studied cases since it is of the first order. This probably happens because the Refs. [2,5] consider the local dissipation (only at the ends

of the chain), while we are interested in the global dissipation. The difference with respect to the transition in Ref. [1] lies in the fact that the NESS is not Gaussian (Gaussianity allows usage of the Wick's theorem for the calculation of higher-order correlation functions in terms of two-point ones, while non-Gaussian states do not allow such expression): in our case the particle-particle correlation functions in the presence of dissipation decay exponentially, while for the  $XX$  chain with on-site dephasing there is a power-law decay of correlations.

The current in the steady dissipative state of the system decays exponentially inside the chain, because the coupling to the environment decreases the coherence of the quantum system. For the random dissipation along the chain, we find that the average current decreases inside the system with the same exponent as for the chain with the same dissipation at every site, which equals to the mean of the random coupling. One can try to measure the current along the dissipative chain with a scanning tunneling microscope (STM): if it decreases exponentially uniformly along the chain, then the dissipation model without disorder is a valid model, if the current inside the chain fluctuates, then the dissipation inside of the chain is random. The STM should be in the regime of a very low tunneling rate to the microscope tip, so that the tunneling to the tip does not destroy the dissipative state of the system itself.

We finish with an outlook. The state of the quantum system depends on the dimensionality, disorder, interaction, statistics, and symmetries. The dissipation adds one more axis to the phase diagram. It can lead to new types of behavior, already investigated in the spin-boson model [10], arrays of the dissipative Josephson junctions, and dissipative spin chains [6–9]. In the present paper we have investigated the behavior of the noninteracting fermionic system coupled to the Markovian bath and already have seen interesting quantum critical phenomena upon adding the dissipation along the chain. There are many unanswered questions: will this transition remain first order upon adding memory to the bath; what happens to it in the presence of interactions; do dimensionality and symmetries influence the behavior of the dissipative system, etc.

## ACKNOWLEDGMENTS

This work was supported through CRC SFB 1073 (Project B03) of the Deutsche Forschungsgemeinschaft (DFG). We are grateful to Achim Rosch and Fabian Biebl for careful reading of the manuscript and helpful discussions.

## APPENDIX: TRANSFORMATION OF THE LIOUVILLIAN TO THE DIAGONAL BASIS

The solution of the Lindblad equation (6) for noninteracting fermions is notably simplified in the super-fermionic representation [21,22]: operators acting from the right on the density matrix are introduced. They are denoted by a tilde. Then the Liouvillian can be written after the particle-hole

transformation  $\tilde{a} = b^\dagger, \tilde{a}^\dagger = b$  in the quadratic form:

$$\mathcal{L} = (a^\dagger b^\dagger) \mathcal{M} \begin{pmatrix} a \\ b \end{pmatrix} - i \sum_{\mu} \Gamma_{\mu}^{(o)} - i \sum_{\mu} \Gamma_{\mu}^{(i)}, \quad (\text{A1})$$

where the matrix  $M$  can be represented as

$$\begin{aligned} \mathcal{M} = & H\delta_{aa} + H\delta_{bb} + i\Gamma_k^{(i)}\delta_{kk}(-\delta_{aa} + \delta_{bb}) \\ & + i\Gamma_k^{(o)}\delta_{kk}(\delta_{aa} - \delta_{bb}) - 2\Gamma_k^{(i)}\delta_{kk}\delta_{ba} + 2\Gamma_k^{(o)}\delta_{kk}\delta_{ab} \end{aligned} \quad (\text{A2})$$

with  $H$  being a tight-binding Hamiltonian of the system,  $\delta_{xy}$  is the Kronecker symbol, for example  $\delta_{aa}$  denotes the upper-left  $L$  by  $L$  part of the matrix  $\mathcal{M}$ ,  $\delta_{kk}$  stands for the diagonal of the matrix in the site space.

Due to this specific structure of  $\mathcal{M}$  the constant terms in the expression (A3) vanish after introducing a new set of the operators  $\{f, f^\dagger, \tilde{f}, \tilde{f}^\dagger\}$  [22] and even more in this basis the Liouvillian becomes diagonal:

$$\mathcal{L}_f = \sum_i \lambda_i f_i^\dagger f_i - \sum_i \lambda_i^* \tilde{f}_i^\dagger \tilde{f}_i. \quad (\text{A3})$$

The operators  $\{f^\dagger, \tilde{f}^\dagger\}$  are dual to the operators  $\{f, \tilde{f}\}$ , but not Hermitian conjugated, though the operators obey anticommutation relations. The operators  $\{f, f^\dagger, \tilde{f}, \tilde{f}^\dagger\}$  are

linear combinations of the operators  $\{a, a^\dagger, \tilde{a}, \tilde{a}^\dagger\}$ :

$$\begin{aligned} a_m^\dagger &= \sum_{k_1} C_{mk_1}^{(1)} f_{k_1}^\dagger + C_{mk_1}^{(2)} \tilde{f}_{k_1}, \\ a_m &= \sum_{k_1} A_{mk_1}^{(1)} f_{k_1} + A_{mk_1}^{(2)} \tilde{f}_{k_1}^\dagger. \end{aligned}$$

The coefficient matrices  $C$  and  $A$  are connected to the matrix of the eigenvectors  $P$  of the matrix  $\mathcal{M}$  (see Ref. [22]):

$$P = \begin{pmatrix} A^{(1)} & A^{(2)} \\ A^{(3)} & A^{(4)} \end{pmatrix}, \quad (P^{-1})^T = \begin{pmatrix} C^{(1)} & C^{(2)} \\ C^{(3)} & C^{(4)} \end{pmatrix}. \quad (\text{A4})$$

In  $P$  the eigenvectors are ordered in the following way: first  $N$  of eigenvectors correspond to eigenvalues with a negative imaginary part, while the second half have a positive imaginary part and are complex conjugated to the first set. All matrices  $A^{(i)}$  and  $C^{(i)}$ ,  $i = 1, \dots, 4$  have dimension  $N \times N$ .

In the  $f$  basis the Liouvillian operator is diagonal, therefore the stationary solution of the Lindblad equation (6) is the vacuum of the operators  $f$ :

$$f|\text{NESS}\rangle = 0, \quad \tilde{f}|\text{NESS}\rangle = 0.$$

It allows us to calculate the expectation values in the NESS: we transform the operator in the  $a$  basis to the  $f$  basis and take its expectation value with respect to the vacuum.

- 
- [1] M. Žnidarič, *J. Stat. Mech.* (2010) L05002; *Phys. Rev. E* **83**, 011108 (2011).
- [2] T. Prosen and I. Pižorn, *Phys. Rev. Lett.* **101**, 105701 (2008).
- [3] C.-E. Bardyn, M. A. Baranov, C. V. Kraus, E. Rico, A. Imamoğlu, P. Zoller, and S. Diehl, *New J. Phys.* **15**, 085001 (2013); O. Viyuela, A. Rivas, and M. A. Martin-Delgado, *Phys. Rev. B* **86**, 155140 (2012).
- [4] H. T. Mebrahtu, I. V. Borzenets, D. E. Liu, H. Zheng, Y. V. Bomze, A. I. Smirnov, H. U. Baranger, and G. Finkelstein, *Nature (London)* **488**, 61 (2012).
- [5] T. Prosen and B. Žunkovič, *New J. Phys.* **12**, 025016 (2010); T. Prosen, *J. Stat. Mech.* (2010) P07020.
- [6] S. Sachdev, P. Werner, and M. Troyer, *Phys. Rev. Lett.* **92**, 237003 (2004).
- [7] P. Werner, Ph.D. thesis, ETH Zürich, 2005.
- [8] S. Pankov, S. Florens, A. Georges, G. Kotliar, and S. Sachdev, *Phys. Rev. B* **69**, 054426 (2004).
- [9] P. Werner, M. Troyer, and S. Sachdev, *J. Phys. Soc. Jpn. Suppl.* **74**, 67 (2005).
- [10] A. J. Leggett, S. Chakravarty, A. T. Dorsey, M. P. A. Fisher, A. Garg, and W. Zwerger, *Rev. Mod. Phys.* **59**, 1 (1987).
- [11] J. Jin, M. W.-Y. Tu, W.-M. Zhang, and Y. J. Yan, *New J. Phys.* **12**, 083013 (2010).
- [12] G. Lindblad, *Rep. Math. Phys.* **10**, 393 (1976).
- [13] H.-P. Breuer and F. Petruccione, *The Theory of Open Quantum Systems* (Oxford University Press, Oxford, 2007).
- [14] Z. Cai and T. Barthel, *Phys. Rev. Lett.* **111**, 150403 (2013).
- [15] Z. Racz, *Nonequilibrium Phase Transitions*, Lecture Notes, Les Houches, July 2002.
- [16] T. Antal, Z. Racz, and L. Sasvari, *Phys. Rev. Lett.* **78**, 167 (1997).
- [17] L. D. Landau and E. M. Lifshitz, *Statistical Physics*, 3rd ed. (Elsevier, Amsterdam, 1980).
- [18] M. Le Bellac, F. Mortessagne and G. G. Batrouni, *Equilibrium and Nonequilibrium Statistical Thermodynamics* (Cambridge University Press, Cambridge, 2004).
- [19] N. Goldenfeld, *Lectures on Phase Transitions and the Renormalization Group* (Perseus, New York, 1992).
- [20] S. Ajisaka, F. Barra, C. Mejia-Monasterio, and Toma Prosen, *Phys. Rev. B* **86**, 125111 (2012).
- [21] A. A. Dzhioev and D. S. Kosov, *J. Chem. Phys.* **134**, 044121 (2011); *J. Phys.: Condens. Matter* **24**, 225304 (2012).
- [22] M. V. Medvedyeva and S. Kehrein, arXiv:1310.4997.
- [23] M. Žnidarič, *Phys. Rev. Lett.* **112**, 040602 (2014).
- [24] K. Maschke and M. Schreiber, *Phys. Rev. B* **49**, 2295 (1994).
- [25] D. Roy and N. Kumar, *Phys. Rev. B* **77**, 064201 (2008).
- [26] M. W. Y. Tu and W.-M. Zhang, *Phys. Rev. B* **78**, 235311 (2008).
- [27] S. A. Gurvitz and Ya. S. Prager, *Phys. Rev. B* **53**, 15932 (1996); S. A. Gurvitz, *ibid.* **57**, 6602 (1998).
- [28] P.-E. Roche, B. Derrida, and B. Douçot, *Eur. Phys. J. B* **43**, 529 (2005).
- [29] I. Perschel and V. Eisler, *J. Phys. A: Math. Theor.* **42**, 504003 (2009).
- [30] F. Evers and A. D. Mirlin, *Rev. Mod. Phys.* **80**, 1355 (2008).
- [31] G. Falkovich, K. Gawędzki, and M. Vergassola, *Rev. Mod. Phys.* **73**, 913 (2001); G. Falkovich, *J. Phys. A: Math. Theor.* **42**, 123001 (2009).
- [32] K. Maschke and M. Schreiber, *Phys. Rev. B* **44**, 3835 (1991); G. Burmeister, K. Maschke, and M. Schreiber, *ibid.* **47**, 7095 (1993).